Steeds (*12*) identified "split peaks" (here called the CDW fundamental and satellite peaks), but they misinterpreted them as evidence that the T phase domain is not striped. In fact, the diffraction data of Withers and Steeds are consistent with the reconstruction in Fig. 3A.

The difference between the striped domain structure implied by our data and the stretched honeycomb structure obtained from the x-ray diffraction work of Tanda *et al.* (*3*, *10*) may be traced to a slight disagreement in the measured CDW wave vectors. Our measurements differ from those of Tanda *et al.* by only a few thousands of a reciprocal lattice vector. The major result of the discrepancy is a rotation of the calculated domain structure by about 27° as well as an increase in the domain width and length. The domain configuration is exceedingly sensitive to the precise values of the CDW wave vectors. However, we can independently test the accuracy of our measured CDW wave vectors by calculating the expected positions of the satellites from the CDW wave vectors alone. The calculated and observed positions agree to within our experimental uncertainties.

The bulk domain configuration derived from our x-ray diffraction data is in close agreement with the surface domain configuration observed by STM. A real-space reconstruction of the surface in-layer domain configuration, from the Fourier components measured by STM, is shown in Fig. 3B. This image was generated with the same reconstruction method used for Fig. 3A. This reconstruction is equivalent to filtering the Fourier transform shown in Fig. 1B at the satellite and CDW peak frequencies and performing an inverse Fourier transformation. With the frequency components due to the defects (Fig. 1A) filtered out, the striped domain configuration is readily apparent in Fig. 3B. The good agreement between Fig. 3A and Fig. 3B is striking.

Because 1T-TaS_2 is both electronically and structurally a quasi–two-dimensional material, it may not seem too surprising that the surface and bulk CDW domain structures agree. In a material with weak interlayer coupling the absence of coupling from one side for a surface layer should not cause a serious perturbation to the CDW. However, x-ray diffraction studies (*1*, *10*) have established a high degree of correlation of the CDW fundamental frequency across layers in the incommensurate (I), NC, and T phases. Therefore, interlayer coupling is significant, yet its absence from one side does not alter the CDW at the surface.

We expect significant interlayer coupling to correlate CDW domains across layers. Because the domain structure arises from the beating of the CDW frequencies with the satellite frequencies, the coherence of the domain structure along the c axis is determined by the coherence of both the CDW and the satellite frequencies. A lower bound for the coherence of each frequency may be obtained from the peak widths. From our Gaussian fits to the CDW and satellite peaks measured by x-ray diffraction, we obtain full width at half-maximum values, projected onto the c* axis, of about 0.035 c* for both cases. Roughly, this implies that domains are correlated across 20 layers in the T phase of 1T-TaS_2. The domain frequency along the c axis is simply the difference, about c*/3, between the c* components of a CDW wave vector and its satellite. Thus, the striped domain configuration exhibits a three-layer stacking.

REFERENCES AND NOTES

1. C. B. Scruby, P. M. Williams, G. S. Parry, *Philos. Mag.* **31**, 255 (1975).
2. S. C. Bayliss, A. M. Ghorayeb, D. R. P. Guy, *J. Phys. C* **17**, L533 (1984).
3. S. Tanda, T. Sambongi, T. Tani, S. Tanaka, *J. Phys. Soc. Jpn.* **53**, 476 (1984).
4. K. Nakanishi, H. Takatera, Y. Yamada, H. Shiba, *ibid.* **43**, 1509 (1977).
5. K. Nakanishi and H. Shiba, *ibid.*, p. 1893.
6. X. L. Wu and C. M. Lieber, *Science* **243**, 1703 (1989).
7. B. Burk, R. E. Thomson, A. Zettl, J. Clarke, *Phys. Rev. Lett.* **66**, 3040 (1991).
8. R. V. Coleman, W. W. McNairy, C. G. Slough, *Phys. Rev. B* **45**, 1428 (1992).
9. K. Nakanishi and H. Shiba, *J. Phys. Soc. Jpn.* **53**, 1103 (1984).
10. S. Tanda and T. Sambongi, *Synth. Metals* **11**, 85 (1985).
11. R. E. Thomson *et al.*, *Phys. Rev. B* **38**, 10734 (1988).
12. R. L. Withers and J. W. Steeds, *J. Phys. C* **20**, 4019 (1987).

13. We thank F. Hollander for valuable assistance with x-ray diffraction. This work was supported by NSF grant DMR-90-17254 (B.B. and A.Z.), and by the Director, Office of Energy Research, Office of Basic Energy Science, Materials Science Division of the U.S. Department of Energy, under contract DE-AC03-76F00098 (R.E.T. and J.C.).

11 March 1992; accepted 26 May 1992

Direct Electrochemical Measurements Inside a 2000 Angstrom Thick Polymer Film by Scanning Electrochemical Microscopy

Michael V. Mirkin, Fu-Ren F. Fan, Allen J. Bard*

An extremely small, conically shaped Pt microelectrode tip (with a radius of 30 nanometers) and the precise positioning capabilities of the scanning electrochemical microscope were used to penetrate a thin (200 nanometers) polymer film and obtain directly the standard potential and kinetic parameters of an electrode reaction within the film. The thickness of the film was determined while it was immersed in and swollen by an electrolyte solution. The film studied was the perfluorosulfonate Nafion containing $Os(bpy)_3^{2+}$ (bpy, 2,2′-bipyridine) cast on an indium tin oxide surface. The steady-state response at the ultramicroelectrode allowed direct determination of the rate constant for heterogeneous electron transfer k° and the diffusion coefficient D without complications caused by transport in the liquid phase, charge exchange at the liquid-polymer interface, and resistive drop.

The advent of ultramicroelectrodes (*1*) has encouraged attempts at electrochemical studies in very small structures, for example, within single biological cells (*2*) or tiny drops of solution (*3*). Such probes are also useful for studying electrochemical processes in thin films. The electrochemistry of films of ionically conducting polymers, such as Nafion, that contain redox species has been studied extensively (*4*, *5*), but questions still remain about the distribution of species and the rates of mass transfer and electron transfer (ET) within the film. The typical experimental approach in such studies involves formation of a polymer film of nanometer to micrometer thickness by spin or drop coating followed by electrochemical studies of the film-substrate region as an electrode in contact with a solution containing one or more redox active species. Alternative structures that have been used include electroactive polymers with metal-sandwich and interdigitated array structures coated on microelectrodes (*6*). The current, determined by the ET rate at the substrate-film interface, can be governed by a number of processes, including diffusion in solution, charge transfer or extraction at the film-solution interface, mass transfer and ET reactions within the film, movement of co-ions, and heterogeneous ET processes at the film-substrate interface. The existence of all of these processes, as well as the added problem of film resistivity, greatly complicates the determination of kinetic parameters (such as k° and D) as functions of film loading with electroactive species and solu-

Department of Chemistry and Biochemistry, University of Texas at Austin, Austin, TX 78712.

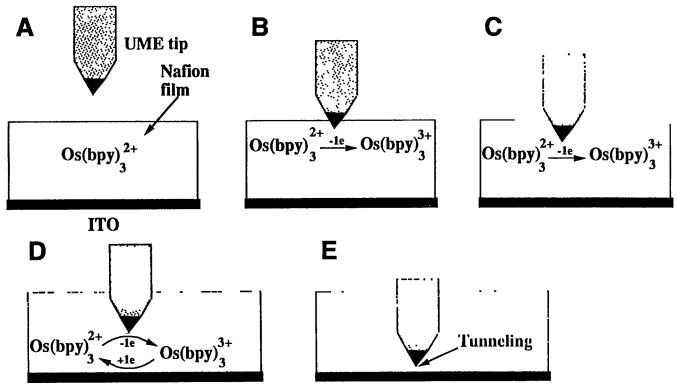

Fig. 1. A scheme representing five stages of the SECM current-distance experiment. (**A**) The tip is positioned in the solution close to the Nafion coating. (**B**) The tip has penetrated partially into Nafion and the oxidation of $Os(bpy)_3^{2+}$ occurs. The effective tip surface grows with penetration. (**C**) The entire tip electrode is in the film but is not close to the ITO substrate. (**D**) The tip is sufficiently close to the substrate to observe positive SECM feedback. (**E**) The tunneling region.

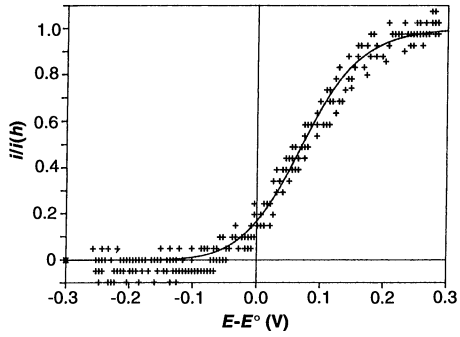

Fig. 3. Voltammogram at a microtip electrode partially penetrating a Nafion film containing 0.57 M $Os(bpy)_3^{2+}$. Scan rate v = 5 mV/s. The solid line is computed by substituting the kinetic parameters given in the text into equation 9 in (*17*).

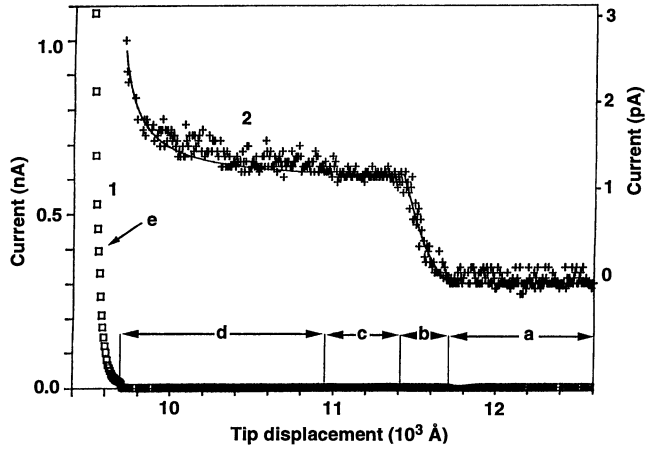

Fig. 2. Dependence of the tip current versus distance. The letters a to e correspond to five stages in Fig. 1. The displacement values are given with respect to an arbitrary zero point. The current observed during stages a to d is much smaller than the tunneling current and therefore cannot be seen on the scale of curve 1 (the left-hand current scale). Curve 2 is at higher current sensitivity to show the current-distance curve corresponding to stages a to d (the right-hand current scale). The solid line is computed for a conically shaped electrode with a height h = 30 nm and a radius, r_0 = 30 nm by Eq. 2 for zones a to c and SECM theory (*14*) for zone d. The tip was biased at 0.80 V versus SCE, and the substrate was at 0.20 V versus SCE. The tip moved at a rate of 30 Å/s.

tion composition (*7*). Of particular interest is how the polymer environment affects $k°$ compared to the same heterogeneous ET reaction in the liquid phase (*8*, *9*).

We used the scanning electrochemical microscope (SECM) (*10*) to study the behavior of a Nafion film containing $Os(bpy)_3^{2+}$ (bpy, 2,2′-bipyridine). Previous SECM studies of polymer films (*11*–*13*) have relied on using the tip to probe the solution environment directly above the polymer to investigate ET and ion ejection and incorporation into the film. In the study reported here, the tip current was recorded as it was moved from the solution into the polymer phase and ultimately contacted the substrate. The interpretation of the current-distance curves [based on an earlier model (*14*)] and an analysis of the voltammograms for the tip inside the film allowed us to evaluate the tip shape and to determine the coating thickness, the kinetic parameters of $Os(bpy)_3^{2+}$ electrooxidation in the Nafion film (that is, D, $k°$, and the transfer coefficient α), and the formal potential $E°'$.

The tip current i was monitored as a function of the relative tip displacement in the direction normal to the film/ITO (indium tin oxide) substrate (*15*, *16*). The experiment was carried out with an aqueous solution of 40 mM $NaClO_4$ as the supporting electrolyte. During the distance scan, the tip was held at 0.80 V versus a saturated calomel electrode (SCE), where $Os(bpy)_3^{2+}$ oxidation is diffusion controlled. The ITO substrate was biased at 0.20 V versus SCE so that any $Os(bpy)_3^{3+}$ generated at the tip that reached the substrate would be reduced back to $Os(bpy)_3^{2+}$ at sufficiently small tip-substrate separations. A scheme of the SECM experiment (Fig. 1) can be represented by five stages: (i) Initially (Fig. 1A) the Pt microtip is in the solution near the Nafion/electrolyte interface. Because the electrolyte contains no electroactive species, a negligibly small current is observed before the tip touches the film surface (see Fig. 2; the portion of the current-distance curve designated a). (ii) When the tip starts to penetrate into the polymer (Fig. 1B), the anodic current increases gradually (Fig. 2b) until it reaches some limiting value. This increase represents the increasing area of the tip exposed to Nafion as the conically shaped Pt penetrates the polymer film. (iii) When the tip is completely immersed in the film, but still "far" (that is, greater than a few tip diameters) from the ITO substrate, the current remains constant and independent of distance. This effect is observed over the interval from 11,400 to 11,000 Å (Fig. 2c). (iv) When the tip gets close to the substrate, the SECM positive feedback effect becomes important and the tip current increases (Fig. 2d). (v) Finally, when the tip gets to within tunneling distance of the substrate, a large increase in current occurs (Fig. 2e). Good reproducibility of successive current-distance curves, obtained with the same tip penetrating either the same or a different portion of the film, indicates that both film and tip are virtually unaffected in this experiment.

The current response as the tip penetrates the film (Fig. 2b) can be used to judge the shape of the tip. The shape of the current-distance curve in this region is consistent with an increase in current due to the growth of the effective electrode surface area, which continues until the entire tip is inside the film. At that point, the effective tip surface area in the film is constant and results in a steady-state current i^∞ that is independent of tip displacement. The ratio of the area of the portion of the conical surface of the tip (*14*) in the film (Fig. 1B) to the total surface area can be expressed by

$$A_e/A = h_e^2/h^2 \quad (1)$$

where h is the height, A is the total surface area of the conical tip, and the subscript "e" designates the effective values for the part of the electrode in the film. Equation 1 results in a parabolic current-distance dependence:

$$i(h) = i^\infty h_e^2/h^2 \quad (2)$$

As shown in Fig. 2, i^∞ = 1.25 pA, and the current increase begins when the tip is just at the film-solution interface, at about 11,730 Å. These values were used to find the best fit between Eq. 2 (solid line in Fig. 2, curve 2) and the experimental data with

h = 30 nm. An alternative equation based on proportionality of $i(h)$ to electrode radius, and thus a linear function of h, could also be applied and yields essentially the same value of h. The magnitude of h found by this curve fitting is in good agreement with the length of the interval b between the onset of current and the plateau in Fig. 2.

The thickness of the Nafion film, L, can be found as a difference in relative displacement between the film-solution interface coordinate (11,730 Å) and that for the onset of tunneling (~9,550 Å, Figs. 1E and 2e), yielding $L \cong 2{,}180$ Å. The error in this determination, which results from neglecting the tunneling distance and uncertainty in the film boundary position, should be within 50 to 100 Å, that is, a relative error within 10%. The SECM determination of polymer film thickness in a liquid is more straightforward than ellipsometry, where the film refractive index must be known, or profilometry, which is not applicable to easily deformed films.

When the tip moved deeper into the film (Fig. 2d), the current began to increase again. This part of the curve can be described in terms of the SECM positive feedback (*10*). The fitting procedure based on SECM with a conical tip and the appropriate working curves [figure 4 in (*14*)] showed r_0 = 30 nm and the height-to-radius ratio equal to 1, that is, h = 30 nm, as found above by a different approach. The diffusion-limited i^∞ at such an electrode should be equal to that for a hemispherical electrode with an equivalent superficial diameter (*17, 18*). The radius of such a hemisphere is $r_h = \pi r_0/(2\sqrt{2})$ = 27 nm. In a solution containing 0.178 M $K_4Fe(CN)_6$ and 2 M KCl the same tip showed a diffusion-limited i^∞ of 1.8 nA at 0.8 V versus SCE. From Eq. 3, taking $D = 6.22 \times 10^{-6}$ cm^2/s (*19*), and where F is Faraday's constant, c^* is $Os(bpy)_3^{2+}$ concentration in the film, and n is the number of electrons in half-reaction, we find the radius of the equivalent hemisphere r_h to be 27 nm, in excellent agreement with the SECM result.

$$i^\infty = 2\pi nFc^*Dr_h \qquad (3)$$

At closer tip-substrate distances a tunneling current was observed (Figs. 1E and 2e). The separation of currents attributable to SECM positive feedback and tunneling is not easy, because the smallest distance in the SECM region (Fig. 2d, curve 2) is about 30 Å.

Voltammetry with the tip in the Nafion (Fig. 2, b and c) was performed to evaluate the kinetic parameters, because, unlike SECM current-distance curves, the steady-state voltammogram is fairly insensitive to the exact shape of the tip, which can be approximated by the equivalent size hemisphere. This approach allows a reasonably accurate evaluation of kinetic parameters (*18*).

The voltammogram of $Os(bpy)_3^{2+}$ electrooxidation in Nafion obtained at a scan rate v = 5 mV/s (Fig. 3) shows a plateau current, $i(h)$ = 0.625 pA, which is substantially lower than the i^∞ value in Fig. 2. In this voltammogram, only a part of the tip electrode was inside the Nafion film (Fig. 2b), so its effective size was smaller than the total tip size determined above. From Fig. 2 one can estimate the effective shape parameters of the electrode: $h_e \cong r_e \cong 21$ nm, corresponding to an equivalent size hemisphere r_h = 18.9 nm (*17, 18*). With $c^* = 5.7 \times 10^{-4}$ mol/cm^3 and the r_h value, Eq. 3 yields $D = 1.2 \times 10^{-9}$ cm^2/s, which is in the range of previous studies (*5, 20*). This value is significantly larger than that reported in (*21*), because the higher loading of $Os(bpy)_3^{2+}$ leads to an increase in the apparent diffusion coefficient (*5, 20*).

The kinetic parameters of the electrode reaction can be evaluated with a simple method we recently proposed (*18*) that requires only knowledge of three experimental parameters, that is, $E_{1/2}$, $E_{1/4}$, and $E_{3/4}$ (which are the half-wave potential and two quartile potentials on the steady-state voltammogram), even with an unknown $E^{\circ\prime}$ value. From the voltammogram of Fig. 3, $|E_{1/4} - E_{1/2}| = 49.5$ mV and $|E_{1/2} - E_{3/4}| = 52$ mV with an accuracy better than ±2 mV. From these values and table 1 in (*19*), we find that $E^{\circ\prime} = E_{1/2} - 71$ mV = 555 mV versus SCE, α = 0.52, and $\lambda = k^\circ r_h/D$ = 0.25; thus $k^\circ = \lambda D/r_h = 1.6 \times 10^{-4}$ cm/s. A good fit between the experimental data and the theoretical curve, calculated with the given set of parameters, confirms the reliability of the results (Fig. 3). This k° value is very close to that reported previously (*8*) for $Ru(bpy)_3^{2+}$ in Nafion.

In order to compare the kinetic parameters found for oxidation of $Os(bpy)_3^{2+}$ in Nafion and in aqueous solution, we applied the same analysis to the voltammogram obtained for a solution containing 1.5 mM $Os(bpy)_3^{2+}$ and 0.5 M Na_2SO_4 with a similar working electrode (*14*) and find k° = 0.16 cm/s, α = 0.57, and $E^{\circ\prime}$ = 577 mV versus SCE. This value for the standard rate constant is consistent with previous results (*22*). The three orders of magnitude decrease in k° in the polymer film compared to the same couple in liquid media, in agreement with previous results (*8, 9*), cannot be caused by additional ohmic drop in the film, because even a film resistance in the gigaohm range would be negligible for currents below 1 pA.

This study has shown how a microtip electrode in an SECM can penetrate a film and be used to extract information about potentials, kinetic parameters, and film thickness. It is also useful in determining the shape of microelectrode tips that are too small to image easily by electron microscopy. Information about the thickness of insulating films in contact with solutions should also be obtainable by addition of an electroactive species to the solution and watching the disappearance of current as the tip penetrates the film until the onset of tunneling. This same approach should be useful in the examination of membranes and small biological structures.

REFERENCES AND NOTES

1. R. M. Wightman and D. O. Wipf, in *Electroanalytical Chemistry*, A. J. Bard, Ed. (Dekker, New York, 1989), vol. 15, pp. 267–353.
2. T. Abe, Y. Y. Lau, A. G. Ewing, *J. Am. Chem. Soc.* **113**, 7421 (1991).
3. P. R. Unwin and A. J. Bard, *Anal. Chem.* **64**, 113 (1992).
4. R. W. Murray, in *Electroanalytical Chemistry*, A. J. Bard, Ed. (Dekker, New York, 1984), vol. 13, pp. 191–368.
5. F. C. Anson, D. N. Blauch, J. M. Saveant, C.-F. Shu, *J. Am. Chem. Soc.* **113**, 1922 (1991), and references therein.
6. C. E. D. Chidsey and R. W. Murray, *Science* **231**, 25 (1986).
7. J. Leddy, A. J. Bard, J. T. Maloy, J. M. Saveant, *J. Electroanal. Chem.* **187**, 207 (1985).
8. J. Leddy and A. J. Bard, *ibid.* **189**, 203 (1985).
9. N. Oyama, T. Ohsaka, M. Kaneko, K. Sato, H. Matsuda, *J. Am. Chem. Soc.* **105**, 6003 (1983).
10. A. J. Bard *et al.*, *Science* **254**, 68 (1991).
11. C. Lee and A. J. Bard, *Anal. Chem.* **62**, 1906 (1990).
12. J. Kwak and F. C. Anson, *ibid.* **64**, 250 (1992).
13. C. Lee and F. C. Anson, *ibid.*, p. 528.
14. M. V. Mirkin, F.-R. F. Fan, A. J. Bard, *J. Electroanal. Chem.*, in press.
15. The microtip preparation and the instrument used for SECM and electrochemical measurements were described previously (*14, 16*). This apparatus (*16*) is capable of both scanning tunneling microscopic (STM) and SECM measurements. The cell contained a Pt counterelectrode and saturated calomel reference electrode (SCE). The tip was an electrochemically etched Pt/Ir 125-μm rod completely coated with Apiezon wax followed by use in an STM mode in air to expose the end (*14*). Nafion coatings were applied to the ITO substrate electrode by spin coating at a rotation speed of 3000 rpm with a photoresist spinner. $Os(bpy)_3^{2+}$ was synthesized according to previously reported procedures [J. G. Gaudiello, P. R. Sharp, A. J. Bard, *J. Am. Chem. Soc.* **104**, 6373 (1982)] and incorporated into the Nafion film by immersing the coated electrode in a 1 mM solution overnight. The quantity of $Os(bpy)_3^{2+}$ incorporated in the coatings was then determined by integrating the voltammetric oxidation wave taken at 5 mV/s (coulometric measurement). The loading, $\chi_{Os^{2+}} = \Gamma_{Os^{2+}}/\Gamma_{SO_4^{2-}}$ (where Γ represents the moles of the indicated ionic species in the coating per square centimeter) was between 0.3 and 0.4.
16. F.-R. F. Fan and A. J. Bard, *J. Electrochem. Soc.* **136**, 3216 (1989).
17. K. B. Oldham and C. G. Zoski, *J. Electroanal. Chem.* **256**, 11 (1988).
18. M. V. Mirkin and A. J. Bard, *Anal. Chem.*, in press.
19. G. Denuault, M. V. Mirkin, A. J. Bard, *J. Electroanal. Chem.* **308**, 27 (1991).
20. M. Sharp, B. Lindhom, E. L. Lind, *ibid.* **274**, 35 (1989).
21. H. S. White, J. Leddy, A. J. Bard, *J. Am. Chem. Soc.* **104**, 4811 (1982).
22. T. Saji and S. Aoyagui, *J. Electroanal. Chem.* **63**, 31 (1975).

23. Support of this research by grants from the National Science Foundation and the Robert A. Welch Foundation is gratefully acknowledged.

10 March 1992; accepted 1 June 1992